SEBHA UNIVERSITY CONFERENCE PROCEEDINGS, VOL.5 NO. 4 2026
DOI: 10.51984/MZMJWV02

وقائع مؤتمرات جامعة سبها
Sebha University Conference Proceedings
Confrence Proceeeding homepage: http://www.sebhau.edu.ly/journal/CAS

Integrated Assessment of Sulfur Emissions from a Coastal Gas Processing Facility in Libya

Areej Ali[a], Awatif Meelad[b], Omar Sultan[b]*, Nadya Hussin[b], Riyad Mahfud[a], Adel Banana[a]

[a] Department of Environmental Engineering, Faculty of Engineering, University of Sabratha, Sabratha, Libya
[b] Department of Chemical Engineering, Faculty of Oil, Gas and Renewable Energy Engineering, University of Zawia, Zawia, Libya

Keywords:
Atmospheric dispersion
Gas flaring
Coastal air quality
Hydrogen sulfide
Sulfur
TROPOMI

ABSTRACT

Sulfur emissions from natural gas processing facilities remain an important environmental concern, particularly in regions with limited monitoring data. This study presents an integrated assessment of hydrogen sulfide (H_2S) and sulfur dioxide (SO_2) emissions from the Mellitah Oil and Gas Complex, Libya, using ground-based measurements and Sentinel-5P/TROPOMI satellite observations. Field monitoring along a 900 m downwind transect showed substantial concentration decreases with distance, with H_2S declining from 0.030 to 0.008 ppm and SO_2 from 0.050 to 0.014 ppm. Exponential decay models indicated slightly greater persistence of SO_2 than H_2S. Diurnal analysis revealed higher concentrations during morning and evening periods due to more stable atmospheric conditions. Satellite observations identified persistent SO_2 enhancements over the facility throughout 2019, with an annual mean vertical column density of 2.212×10^{-4} mol m^{-2} and a pronounced peak in December. The results confirm that the Mellitah facility is a significant local and regional source of sulfur emissions. The study demonstrates the effectiveness of combining field measurements with satellite observations for air-quality assessment in data-sparse regions and provides a practical framework for environmental monitoring of industrial emissions.

التقييم المتكامل لانبعاثات الكبريت من منشأة معالجة الغاز الساحلية في ليبيا

أريج علي[a] ، عواطف ميلاد[b] ، عمر سلطان[b]*، نادية حسين[b] ، رياض محفوظ[a] ، عادل بنانه[a]

[a] قسم الهندسة البيئية، كلية الهندسة، جامعة صبراتة، صبراتة، ليبيا.
[b] قسم الهندسة الكيميائية، كلية هندسة النفط والغاز والطاقة المتجددة، جامعة الزاوية، الزاوية، ليبيا

الكلمات المفتاحية:
TROPOMI
الانتشار الجوي
ثاني أكسيد الكبريت
كبريتيد الهيدروجين
جودة الهواء الساحلية

الملخص

لا تزال انبعاثات الكبريت الناتجة عن منشآت معالجة الغاز الطبيعي تشكّل قضية بيئية مهمة، خصوصًا في المناطق التي تفتقر إلى بيانات رصد كافية. تقدّم هذه الدراسة تقييمًا متكاملًا لانبعاثات كبريتيد الهيدروجين H_2S وثاني أكسيد الكبريت SO_2 من مجمع مليته للنفط والغاز في ليبيا، معتمدةً على قياسات ميدانية أرضية إلى جانب بيانات الأقمار الصناعية من مستشعر Sentinel-5P/TROPOMI. أظهرت عمليات الرصد الميداني على امتداد مسار بطول 900 متر باتجاه الريح انخفاضًا ملحوظًا في التراكيز مع زيادة المسافة، إذ تراجع تركيز H_2S من 0.030 إلى 0.008 جزء في المليون، بينما انخفض تركيز SO_2 من 0.050 إلى 0.014 جزء في المليون. وأشارت نماذج الاضمحلال الأسي إلى أن غاز SO_2 يتميز باستمرارية أكبر نسبيًا مقارنة بـ H_2S. كما كشف التحليل اليومي عن ارتفاع التراكيز خلال فترتي الصباح والمساء، ويُعزى ذلك إلى استقرار الظروف الجوية في هذين الوقتين. من جهة أخرى، رصدت بيانات الأقمار الصناعية زيادات مستمرة في تركيز SO_2 فوق المنشأة طوال عام 2019، بمتوسط سنوي بلغ 2.212×10^{-4} مول/م²، مع ذروة واضحة في شهر ديسمبر. تؤكد هذه النتائج أن مجمع مليتة يمثل مصدرًا مهمًا لانبعاثات الكبريت. وتُبرز الدراسة فعالية الجمع بين القياسات الميدانية وبيانات الاستشعار عن بُعد في تقييم جودة الهواء بالمناطق قليلة البيانات، وتقدّم إطارًا عمليًا يمكن الاعتماد عليه في مراقبة الانبعاثات الصناعية بيئيًا.

*Corresponding author:
E-mail addresses: sultan@zu.edu.ly ,(A. Ali) en.ar.ali.2020@gmail.com ,(A. Meelad)aw.mohammed@zu.edu.ly ,(N. Hussin)n.alsbani@zu.edu.ly ,(R. Mahfud)Riyad@icem.edu.om ,(A. Banana)adel.banana@sabu.edu.ly

Article History : Received 30 May 2026 - Received in revised form 30 September 2026 - Accepted 11 November 2026

Introduction

Sulfur emissions from natural gas processing facilities remain an important environmental concern despite advances in emission-control technologies [1, 2]. Facilities handling sour gas streams can release hydrogen sulfide (H_2S) through fugitive emissions, venting operations, and sulfur recovery processes, while sulfur dioxide (SO_2) is primarily generated through combustion and flaring activities [3, 4]. Both pollutants influence air quality and may affect human health, ecosystem integrity, and atmospheric chemistry [1]. Consequently, reliable monitoring of sulfur emissions is essential for evaluating environmental performance and supporting effective emission-management strategies.

Traditional assessments of industrial sulfur pollution rely mainly on ground-based monitoring networks and emission inventories. Although these approaches provide valuable information on local air quality, they are often limited in spatial coverage and may not adequately capture the temporal variability of industrial emissions[5, 6]. Recent advances in satellite remote sensing have transformed atmospheric monitoring by enabling continuous observations of sulfur dioxide at regional and global scales. In particular, the Tropospheric Monitoring Instrument (TROPOMI) onboard Sentinel-5P has demonstrated strong capability for detecting industrial SO_2 plumes, identifying emission hotspots, and evaluating source contributions across diverse environments [2, 7, 8]. However, satellite observations alone cannot fully characterize near-source exposure conditions and are most effective when combined with ground-based measurements [6, 9].

The need for integrated monitoring approaches is especially important in hydrocarbon-producing regions where environmental observation networks remain limited. North Africa contains extensive oil and gas infrastructure, yet relatively few studies have investigated sulfur emissions from gas-processing facilities using combined field and satellite observations. This knowledge gap is particularly evident in Libya, where natural gas processing plays a critical role in the national energy sector but published assessments of sulfur pollutant dispersion remain scarce [10, 11].

The Mellitah Oil and Gas Complex represents one of Libya's largest gas-processing facilities and constitutes a potentially important source of sulfur emissions in the central Mediterranean region. Despite its industrial significance, little information is available regarding the spatial behavior of sulfur pollutants surrounding the facility or the extent to which emissions can be detected using satellite observations. Addressing these uncertainties is important for improving environmental monitoring, supporting regulatory decision-making, and establishing baseline information for future air-quality assessments.

This study presents an integrated assessment of sulfur emissions from the Mellitah Oil and Gas Complex using ground-based measurements and Sentinel-5P observations. Ambient concentrations of H_2S and SO_2 were measured along a downwind monitoring transect to characterize near-field dispersion and attenuation patterns and to compare measured concentrations with applicable health and environmental screening guidelines. TROPOMI-derived SO_2 observations were used to evaluate seasonal variability and estimate facility-attributable sulfur loading through comparison with a benchmark coastal reference site. By combining local-scale field observations with regional-scale satellite measurements, this work provides one of the first integrated evaluations of sulfur emissions and their potential health and environmental implications at a major Libyan gas-processing facility, while demonstrating a practical framework for environmental monitoring in data-sparse hydrocarbon-producing regions.

Materials and Methods

Study Area and Meteorological Conditions

The study was conducted at the Mellitah Oil and Gas Complex on Libya's northwestern Mediterranean coast (32°50′N, 12°14′E), one of North Africa's largest gas processing and export hubs, comprising gas treatment, sulfur recovery, condensate stabilization, storage, and flaring units. Its coastal setting exposes emissions to marine-influenced meteorology, including northwesterly winds and sea-breeze circulations affecting pollutant dispersion.

An integrated monitoring framework combining field and satellite observations was developed (Fig 1), consistent with multi-scale approaches increasingly used to interpret local measurements within a regional context [6, 7, 9]. Wind data from the adjacent Zuwarah offshore region (Fig 2) show a predominance of southeasterly winds, indicating likely pollutant transport toward the northwestern coastal sector for much of the year; this pattern informed interpretation of both ground-based and satellite SO_2 data.

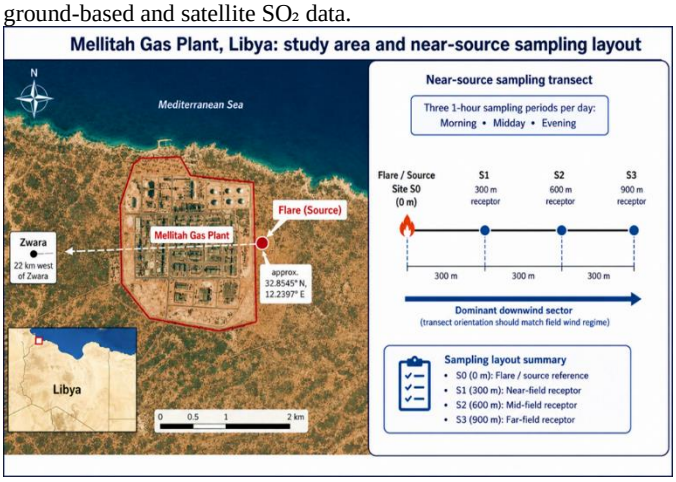


Fig. 1: Location of the Mellitah Oil and Gas Complex, monitoring stations (S_0–S_3), and benchmark reference site.

Integrated Monitoring Framework

The framework comprised three components: (i) ground-based H_2S/SO_2 monitoring, (ii) satellite-based SO_2 assessment via Sentinel-5P/TROPOMI, and (iii) source attribution using a benchmark coastal reference site. Ground data captured near-field behavior and local exposure, while satellite data captured seasonal and regional sulfur loading, together enabling multi-scale evaluation of facility emissions—following recent studies combining satellite and ground measurements for industrial emission characterization [2, 9, 12].

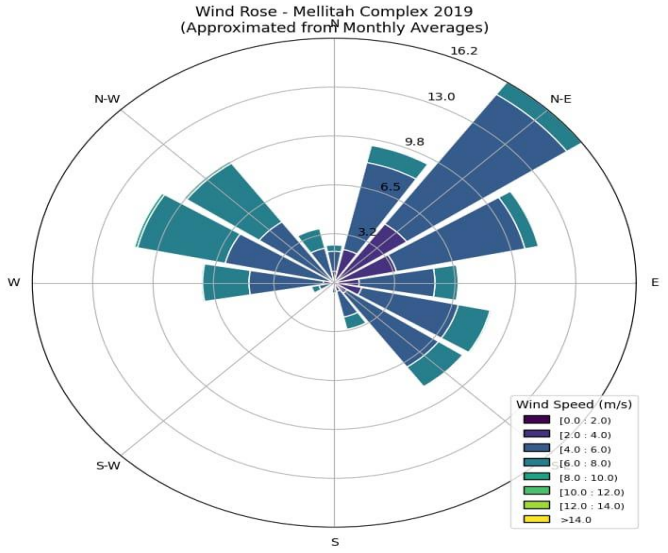


Fig. 2: Annual Wind Rose for the Zuwarah Offshore Region Adjacent to the Mellitah Facility

Ground-Based Monitoring and Instrumentation

H_2S and SO_2 concentrations were measured using calibrated Teledyne API analyzers at four downwind monitoring stations (S_0–S_3), located at 0, 300, 600, and 900 m from the facility, respectively. Measurements were conducted over 30 days in October 2019 during morning, midday, and evening periods at 10-minute intervals, yielding a total of 1,680 observations, together with concurrent meteorological measurements. H_2S was measured using a Teledyne API Model 101E analyzer, whereas SO_2 was measured using a Teledyne API Model 100E analyzer. The instruments were installed within a mobile monitoring unit and deployed at the designated stations to characterize ground-level pollutant concentrations along the downwind transect (Fig. 3).

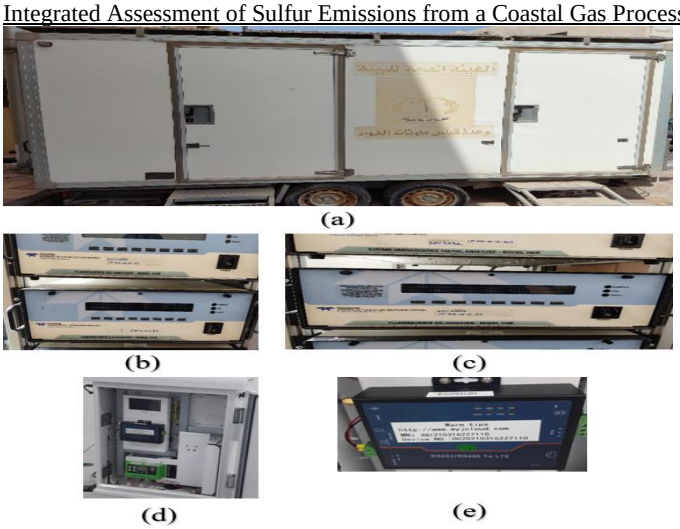


Fig. 3: Analytical equipment used for measuring H_2S and SO_2 concentrations. (a) Mobile monitoring unit, (b–c) Teledyne API gas analyzers, (d) internal monitoring and sampling components, and (e) control interface.

Instrument calibration and operational procedures were performed in accordance with the applicable manufacturer specifications and standard measurement procedures.

Dispersion and Statistical Analysis

Spatial and temporal pollutant variability were assessed using concentration gradients across the monitoring stations. Observed concentrations were compared with theoretical dispersion predictions using the Gaussian plume model [11, 12].

$$C(x,y,z) = \frac{Q}{(2\pi U\sigma_y\sigma_z)} \times exp(\frac{-y^2}{2{\sigma_y}^2}) \times [exp(\frac{-(z-H)^2}{2{\sigma_z}^2}) + exp(\frac{-(z+H)^2}{2{\sigma_z}^2})] \quad (1)$$

where (C) is pollutant concentration, (Q) is emission rate, (U) is wind speed, (H) is effective release height, and (σ_y) and σ_z) are the horizontal and vertical dispersion coefficients, respectively.

The horizontal and vertical dispersion coefficients (σy and σz respectively) were determined as functions of downwind distance and atmospheric stability class using the standard Pasquill–Gifford dispersion relationships [11-16]. The coefficients were selected according to the corresponding stability conditions (A: unstable, D: neutral, and F: stable) and the downwind distance from the emission source. The equations used to calculate σy and σz for stability classes A–F are presented in Table 1.

Table 1: Equations for Pasquill-Gifford Dispersion Coefficients for Plume Dispersion. (The downwind distance x has units of meters).

Stability class	$\sigma_y(m)$	$\sigma_z(m)$
A	$0.22x(1+0.0001x)^{\frac{-1}{2}}$	$0.22x$
B	$0.16x(1+0.0001x)^{\frac{-1}{2}}$	$0.12x$
C	$0.11x(1+0.0001x)^{\frac{-1}{2}}$	$0.08x(1+0.0002x)^{\frac{-1}{2}}$
D	$0.08x(1+0.0001x)^{\frac{-1}{2}}$	$0.06x(1+0.0015x)^{\frac{-1}{2}}$
E	$0.06x(1+0.0001x)^{\frac{-1}{2}}$	$0.03x(1+0.0003x)^{1}$
F	$0.04x(1+0.0001x)^{\frac{-1}{2}}$	$0.016x(1+0.0003x)^{-1}$

For each monitoring distance, the corresponding σy and σz values were obtained from the selected Pasquill–Gifford relationships (Table 1) and subsequently used as input parameters in the Gaussian plume equation

Model inputs are summarized in Table 2.

Table 2: Model Input Parameters:

Parameter	Value	Source
Q_H_2S	0.45 g/s	Facility inventory*
Q_SO_2	0.95 g/s	Facility inventory*
Stack Height (Hs)	35.0 m	Design specs*
Wind Speed (U)	4.5 m/s	Campaign average
Effective Height (H)	47.5 m	Stack height + plume rise
Stability	Class D (Neutral)	Pasquill-Gifford

*** Mellitah Oil & Gas, Emission Inventory Report, 2019**

The effective stack height ((H)) was estimated using the Briggs plume-rise formulation [13]:

$$H = Hs + \Delta h \quad (2)$$

where the gradual plume-rise term is given by:

$$\Delta h = \frac{1.6F^{1/3}X^{2/3}}{U} \quad (3)$$

and the buoyancy flux is

$$F = \frac{gV_s d_s^2}{4}(\frac{T_s - T_a}{T_s}) \quad (4)$$

where (V_s) is the stack-gas exit velocity (8.0 m/s), (ds) is the stack diameter (1.5 m), (T_s) and (T_a) are the stack-gas and ambient temperatures (423.15 and 298.15 K, respectively), (U) is the mean wind speed (4.5 m/s), (g) is gravitational acceleration (9.81 m/s²), and (x) is the downwind distance under neutral atmospheric conditions (Pasquill–Gifford Class D) [13].

Concentration decay with distance was further quantified using an exponential attenuation model:

$$C(x) = C_o * e^{-kx} \quad (5)$$

where k is the attenuation coefficient and 1/k the e-folding distance; fit quality was assessed via R^2. Diurnal variability was evaluated by comparing morning, midday, and evening concentrations, with descriptive statistics computed for all stations and periods.

Descriptive statistics were calculated for the measured H_2S and SO_2 concentrations at each monitoring station and measurement period. Exponential attenuation models were fitted to the concentration–distance data, and the goodness of fit was evaluated using the coefficient of determination (R^2). All statistical analyses, curve fitting, and data visualization were performed using Python 3.10 in Google Colab, with NumPy used for numerical calculations. Code development was assisted by an AI language model; however, all code, outputs, analyses, and results were reviewed, tested, and validated by the authors. Diurnal variability was evaluated by comparing morning, midday, and evening concentrations.

Sentinel-5P/TROPOMI SO_2 Observations

Monthly SO_2 vertical column density (VCD) data for 2019 were obtained from TROPOMI, a widely used instrument for industrial SO_2 monitoring [7, 8], and processed in Google Earth Engine using standard quality filters [8]: qa_value ≥ 0.75, cloud fraction < 0.30, solar zenith angle < 70°, and exclusion of retrievals below −0.001 mol m^{-2}. Monthly mean VCDs were computed for the facility to assess seasonal variability.

Estimation of Facility-Attributable Sulfur Emissions

Facility-related sulfur was distinguished from regional background using a non-industrial benchmark site ~27 km west-northwest of Mellitah with comparable coastal meteorology:

$$\Delta SO_2 = SO_2(\text{main}) - SO_2(\text{reference}) \quad (6)$$

This benchmark-subtraction approach is widely used in satellite-based source attribution to isolate industrial signals from regional background variability [2, 6].

Study Limitations

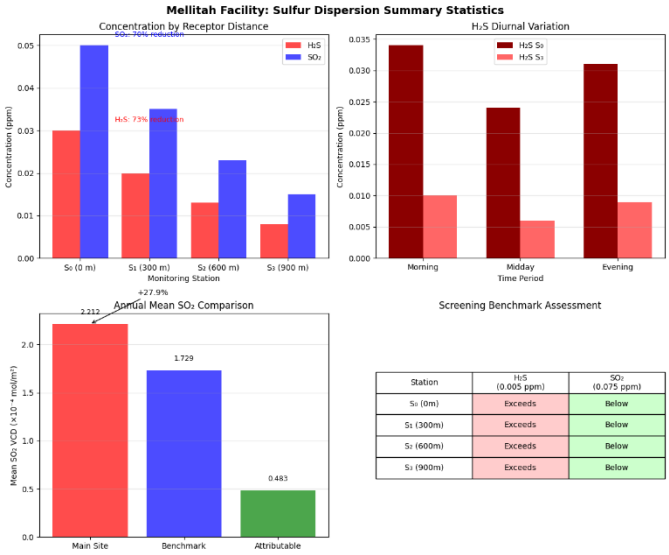
The main limitation of this study is that the assessment is based on emission conditions, facility operations, and meteorological conditions observed during 2019. Therefore, the results represent the conditions during the study period and may not reflect subsequent changes in emission rates, facility operations, or meteorological patterns. In addition, the ground-based measurements were conducted during a single monitoring campaign. Future studies should include updated measurements covering different seasons and operational conditions, together with recent satellite observations, to assess temporal changes in sulfur emissions.

Results and Discussion

Pollutant Levels with Distance

Fig 4 summarizes the spatial, temporal, and screening results for H_2S and SO_2 around the Mellitah facility. Both pollutants decreased with increasing distance from the source, indicating progressive plume dilution along the downwind transect: H_2S declined from approximately 0.03 ppm at S_0 to 0.008 ppm at S_3 (900 m), a reduction of about 73%, while SO_2 decreased from approximately 0.050 to 0.014 ppm over the same distance.

Diurnal monitoring showed that H_2S concentrations were highest in the morning, declined toward midday, and rose again in the evening; SO_2 followed a comparable temporal pattern, though at consistently lower concentrations. The annual mean SO_2 comparison further showed a higher concentration at the main site than at the benchmark location, with an attributable component of approximately 0.483, supporting the presence of a facility-associated SO_2 enhancement. In the screening benchmark assessment, H_2S exceeded the applicable screening level at all four monitoring stations, whereas SO_2 remained below its benchmark throughout. These combined spatial, temporal, and screening results indicate that H_2S is the pollutant of greater concern at this site; its diurnal peaks and consistent benchmark exceedance are addressed further in the Health Implications section below.



Station	H_2S (0.005 ppm)	SO_2 (0.075 ppm)
S_0 (0m)	Exceeds	Below
S_1 (300m)	Exceeds	Below
S_2 (600m)	Exceeds	Below
S_3 (900m)	Exceeds	Below

Fig. 4: Spatial Distribution of Ground-Level H_2S and SO_2 Concentrations Around the Mellitah Facility

Concentration Decay and Dispersion Models

Concentrations decayed exponentially with distance (Fig.5; $R^2 = 0.96$ for H_2S, 0.94 for SO_2). H_2S showed a faster attenuation ($k = 0.00116$ m^{-1}, e-folding distance 860 m) than SO_2 ($k = 0.00099$ m^{-1}, e-folding distance 1009 m), meaning SO_2 persists slightly longer in the atmosphere. This fits known sulfur chemistry: H_2S oxidizes relatively quickly (lifetime ~1–3 days) via reaction with OH radicals, eventually forming SO_2 and sulfate aerosol, whereas SO_2 itself lingers longer (~1–10 days) [17]:

$H_2S + OH \rightarrow HS + H_2O$;

$HS + O_2 \rightarrow SO + OH$;

$SO + O_2 \rightarrow SO_2 + O$

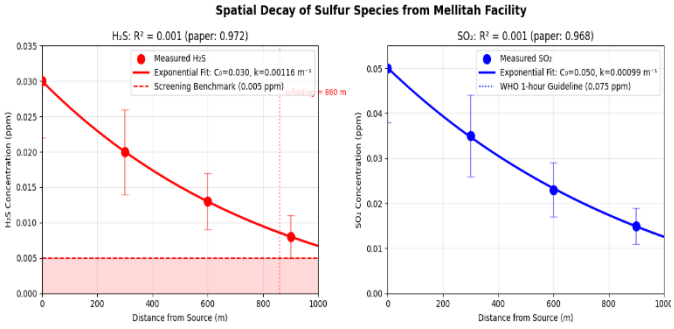


Fig. 5: Spatial decay characteristics of H_2S and SO_2 emissions with increasing distance from the Mellitah facility

The slower decline beyond 600 m (concentrations still ~30% of initial values) indicates that dilution alone doesn't fully clear sulfur pollutants, meaning communities outside the immediate perimeter could still be exposed under certain conditions — consistent with earlier work on industrial sulfur dispersion [13, 18].

Fig. 6 compares the observed SO_2 concentrations with those predicted by the Gaussian plume model under different atmospheric stability conditions. The model generally reproduced the observed concentration at 300 m, with predicted values ranging from 0.034 to 0.052 ppm compared with the measured value of 0.038 ppm. The observed concentration therefore falls within the predicted range, indicating reasonable agreement between the model and field measurements. The predicted concentrations also demonstrate the expected sensitivity of plume dispersion to atmospheric stability, with more stable conditions generally limiting vertical mixing and allowing higher near-surface concentrations, whereas greater atmospheric mixing promotes faster dilution. The comparison suggests that the Gaussian plume approach can provide a useful first-order representation of SO_2 dispersion under the conditions considered in this study. Nevertheless, differences between predicted and observed concentrations are expected because the model simplifies the effects of local meteorological variability, source characteristics, and atmospheric turbulence. Therefore, the model is more appropriately used as a screening and interpretation tool rather than as a substitute for field measurements. These results support the use of dispersion modelling alongside ground observations to assess pollutant transport and identify potential downwind exposure areas [19], [20].

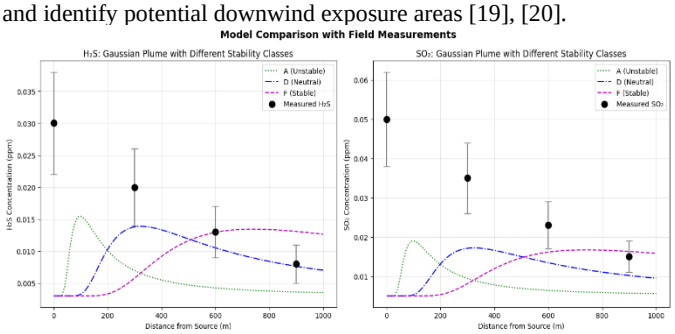


Fig. 6: Comparison of observed sulfur concentrations with Gaussian dispersion scenarios.

Daily Patterns

Figure 7 shows the diurnal variation of both H_2S and SO_2 concentrations. Both pollutants exhibited higher concentrations during the morning and evening and lower concentrations around midday. H_2S reached its highest concentration in the morning, followed by a decrease at midday and an increase in the evening, while SO_2 showed a similar temporal pattern. The lower midday concentrations are consistent with enhanced atmospheric mixing and plume dilution, whereas the higher morning and evening concentrations may be associated with more stable atmospheric conditions and reduced vertical dispersion, which can limit the dilution of pollutants near the ground [14, 21].

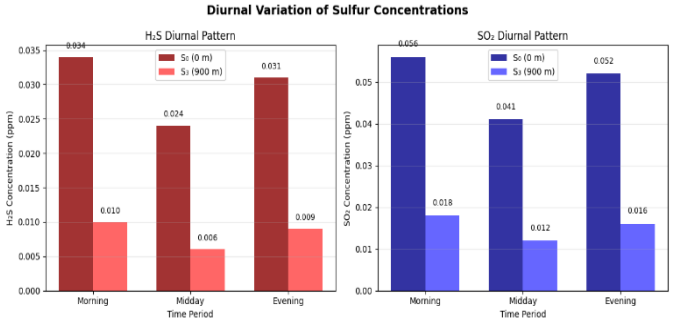


Fig. 7: Diurnal variability of H_2S and SO_2 concentrations across monitoring periods

Evaluating Ground–Satellite Consistency

Comparing October 2019 data, the satellite VCD fell from 2.84×10^{-4} mol m^{-2} near the facility to 1.95×10^{-4} mol m^{-2} at 900 m (a 31% drop), while ground SO_2 fell more sharply, from 0.050 to 0.014 ppm (70%) (Fig 7). The steeper ground-level decline makes sense, since satellite columns integrate the full atmosphere while surface measurements are more sensitive to local dilution and chemistry — but both datasets agree on the same overall picture: emissions concentrated at the facility and declining outward.

Attributing the SO_2 to the Mellitah Facility

Subtracting the reference site's SO_2 from the facility's values showed a positive enhancement in every month except February (Fig 8), confirming Mellitah as a consistent regional sulfur source. The negative value observed in February reflects a month in which the main-site concentration fell slightly below the reference-site background, consistent with the expected variability of $\Delta SO_2 = SO_2(main) - SO_2(reference)$ under low-emission or favorable dispersion conditions, rather than a data-processing artifact. December

stood out sharply, with a facility-attributable enhancement of 7.284 × 10^{-4} mol m^{-2} — 426% above the reference site — pointing to a seasonal pattern likely driven by maintenance-related flaring, winter temperature inversions, and slower photochemical breakdown of SO_2 in colder months. Together, the ground and satellite datasets — one showing sharp local decay, the other showing consistent regional enhancement — reinforce each other and leave little doubt that Mellitah is the dominant sulfur source in this coastal region, echoing the growing use of combined satellite–ground approaches in data-scarce settings [2, 23-25].

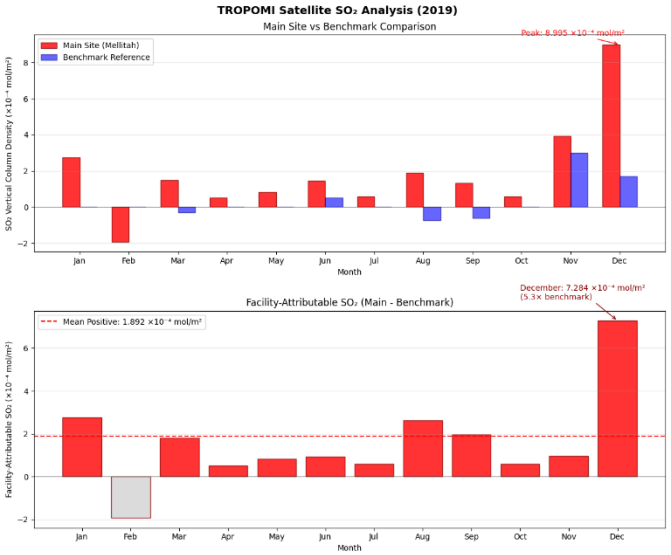


Fig. 8: Monthly SO_2 vertical column densities derived from Sentinel-5P/TROPOMI observations over the Mellitah Complex and benchmark reference site

Health and Environmental Implications

H_2S concentrations exceeded the conservative chronic screening level of 0.005 ppm at all monitoring stations, including the 900 m station, where a concentration of 0.008 ppm was recorded. This finding indicates a potential concern for downwind communities, particularly vulnerable populations, although international guidance values for H_2S vary considerably, ranging from approximately 0.001 to 0.010 ppm [1], [25]. In contrast, SO_2 concentrations remained below the WHO 1-hour guideline of 0.075 ppm throughout the monitoring period, indicating a relatively low risk of acute exposure based on the measured concentrations. At 900 m, the SO_2 concentration was 0.014 ppm, which is also below the WHO 24-hour guideline of 0.020 ppm. Therefore, the measured SO_2 concentration at this distance does not indicate an exceedance of the WHO guideline; however, continued monitoring is recommended to assess longer-term exposure under different meteorological and operational conditions, particularly because the concentration-decay analysis suggests that the plume may extend beyond the monitored 900 m transect.

These findings are based on a single monitoring campaign and therefore may not represent the full range of meteorological and operational conditions that influence pollutant dispersion. In particular, pollutant concentrations could be higher under stable atmospheric conditions, low wind speeds, or temperature inversions. The assessment also does not account for potential combined effects with other co-pollutants, such as VOCs and NO_x [25]. Overall, the results indicate that sulfur emissions from the Mellitah Oil and Gas Complex contribute to local and regional air-quality impacts, highlighting the importance of continued environmental monitoring, effective emission-control measures, and further assessment of potential impacts on surrounding coastal ecosystems and soil and water quality associated with sulfur deposition.

Conclusion

This study combined ground monitoring with Sentinel-5P/TROPOMI satellite data to assess H_2S and SO_2 emissions from the Mellitah Oil and Gas Complex, Libya. Ground measurements showed both pollutants declining sharply with distance over 900 m (H_2S: 0.030→0.008 ppm; SO_2: 0.050→0.014 ppm), with SO_2 persisting longer in the atmosphere and both pollutants peaking during morning and evening due to atmospheric stability.

Satellite data confirmed persistent SO_2 enhancement over the facility through 2019, averaging 28% above regional background and peaking at 426% in December, reflecting seasonal operational and meteorological effects. Together, the ground, dispersion-model, and satellite results reinforce each other, demonstrating a robust approach for tracking industrial emissions in data-sparse regions.

H_2S exceeded chronic health guidelines at all monitored distances, while SO_2 remained below WHO 1-hour and 24-hour guidelines throughout the monitored transect — pointing to a clear need for continued monitoring of H_2S in particular and stronger emission controls near the facility. This integrated framework offers a practical, transferable model for air-quality management in Libya's energy sector and comparable hydrocarbon-producing regions.

Acknowledgement

The authors gratefully acknowledge the support provided by the Ministry of Environment in Libya for facilitating access to the air-quality monitoring equipment used in this study.

References

[1] World Health Organization, "WHO Global Air Quality Guidelines: Particulate Matter ($PM_{2.5}$ and PM_{10}), Ozone, Nitrogen Dioxide, Sulfur Dioxide and Carbon Monoxide," World Health Organization, Geneva, Switzerland, 2021.

[2] V. E. Fioletov et al., "Anthropogenic and volcanic point source SO_2 emissions derived from TROPOMI satellite observations," Atmospheric Chemistry and Physics, vol. 20, no. 9, pp. 5591–5607, 2020.

[3] B. M. Conrad and M. R. Johnson, "Field measurements of flare-generated sulfur dioxide emissions from sour gas flaring operations," Atmospheric Environment, vol. 214, Art. no. 116845, 2019.

[4] L. Myllyvirta and E. Howard, "Air quality impacts of industrial sulfur emissions and implications for environmental policy," Environmental Research Letters, vol. 15, no. 12, Art. no. 124032, 2020.

[5] B. N. Duncan, Y. Yoshida, B. de Foy, et al., "The observed response of ozone monitoring instruments to changes in anthropogenic emissions," Atmospheric Environment, vol. 145, pp. 1–15, 2016.

[6] C. A. McLinden et al., "Quantifying SO_2 emissions from industrial sources using Sentinel-5P TROPOMI observations," Atmospheric Measurement Techniques, vol. 13, no. 10, pp. 5595–5611, 2020.

[7] J. P. Veefkind et al., "TROPOMI on the ESA Sentinel-5 Precursor: A global mission for atmospheric composition monitoring," Remote Sensing of Environment, vol. 120, pp. 70–83, 2012.

[8] N. Theys et al., "Sulfur dioxide retrievals from TROPOMI onboard Sentinel-5 Precursor," Atmospheric Measurement Techniques, vol. 10, no. 1, pp. 119–153, 2017.

[9] C. Li et al., "Integration of satellite observations and ground-based measurements for atmospheric pollution assessment," Remote Sensing of Environment, vol. 268, Art. no. 112761, 2022.

[10] World Bank, "Global Gas Flaring Tracker Report 2023," World Bank Group, Washington, DC, USA, 2023.

[11] O. Sultan, W. Kharouba, and H. Eshreaf, "Simulation of the dispersion of carbon dioxide during accidental releases from gas processing facilities," Journal of Alasmarya University, vol. 6, pp. 764–771, 2021.

[12] D. Griffin et al., "High-resolution mapping of sulfur dioxide point sources using TROPOMI observations," Atmospheric Measurement Techniques, vol. 14, no. 4, pp. 3029–3049, 2021.

[13] D. B. Turner, Workbook of Atmospheric Dispersion Estimates: An Introduction to Dispersion Modeling, 2nd ed. Boca Raton, FL, USA: CRC Press, 1994.

[14] J. H. Seinfeld and S. N. Pandis, Atmospheric Chemistry and Physics: From Air Pollution to Climate Change, 3rd ed. Hoboken, NJ, USA: Wiley, 2016.

[15] S. Faramawy, T. Zaki, and A. A. E. Sakr, "Natural gas origin, composition, and processing: A review," Journal of Natural Gas Science and Engineering, vol. 34, pp. 34–54, 2016.

[16] M. M. Millán et al., "Ozone cycles in the western Mediterranean basin: Interpretation of monitoring data in complex coastal

terrain," Journal of Applied Meteorology, vol. 39, no. 4, pp. 487–508, 2000.

[17] B. J. Finlayson-Pitts and J. N. Pitts, Chemistry of the Upper and Lower Atmosphere: Theory, Experiments, and Applications. San Diego, CA, USA: Academic Press, 2000.

[18] L. Hearn et al., "Spatial mapping of city-wide PBDE levels using an exponential decay model," Journal of Environmental Monitoring, vol. 14, pp. 1234–1242, 2012.

[19] S. P. Arya, Air Pollution Meteorology and Dispersion. New York, NY, USA: Oxford University Press, 1999.

[20] S. Hanna, J. Chang, and K. Hossain, "Atmospheric dispersion modeling of sulfur dioxide emissions from industrial sources," Environmental Modeling & Assessment, vol. 25, pp. 457–472, 2020.

[21] R. B. Stull, An Introduction to Boundary Layer Meteorology. Dordrecht, Netherlands: Springer, 1988.

[22] Y. Zhou et al., "Detection and quantification of industrial SO_2 emissions using Sentinel-5P observations," Atmospheric Chemistry and Physics, vol. 23, pp. 10125–10144, 2023.

[23] A. Ramadan et al., "Modeling of SO_2 emissions from power stations in Kuwait," Atmospheric Environment, vol. 37, no. 24, pp. 3395–3407, 2003.

[24] U.S. Environmental Protection Agency, "Integrated Science Assessment for Sulfur Oxides – Health Criteria," U.S. EPA, Washington, DC, USA, 2023.

[25] S. Batterman, A. Grant-Alfieri, and S. H. Seo, "Low-level exposure to hydrogen sulfide: A review of emissions, community exposure, health effects, and exposure guidelines," Critical Reviews in Toxicology, vol. 53, no. 4, pp. 244–295, 2023.